

# The Master Failure Curve of Pipe Steels and Crack Paths in Connection with Hydrogen Embrittlement

M. Hadj Meliani<sup>1,2,\*</sup>, A. Elhussein<sup>2</sup>, A. Elhoud<sup>3</sup>, Z. Azari<sup>2</sup>, Y.G. Matvienko<sup>4</sup>, G. Pluvinage<sup>2</sup> T. Boukharouba<sup>5</sup>

<sup>1</sup> LPTPM, FS, Hassiba BenBouali University of Chlef, 02000, Chlef, Algeria.

<sup>2</sup> LaBPS-ENIM, Ile de saulcy 57045, Paul Verlaine university of Metz, France.

<sup>3</sup> Sinal, Materials and metallurgical services division, Rue de Madrid, Annaba, Algeria.

<sup>4</sup> Mechanical Engineering Research, 4.M. Kharitonievsky Per., 101990 Moscow, Russia.

<sup>5</sup> Laboratoire de Mécanique Avancée, LMA, USTHB, Algeries, Algeria.

\* Corresponding author: [hadjmeliani@univ-metz.fr](mailto:hadjmeliani@univ-metz.fr)

**Abstract** This paper provides some critical review of the history and state of two elastic fracture mechanics (K and T) and relationship to crack paths. A particular attention is given in the case of hydrogen embrittlement. A fracture toughness transferability curve ( $K_{pc}$ - $T_{ef}$ ) has been established for the X52 pipe steels described by a linear relationship where  $T_{ef}$  is the average value of T stress over the characteristic length of the fracture process. A mechanism involving influence of the  $T_{ef,c}$ -stress on void growth for ductile failure is proposed; the effects of hydrogen on crack paths from the viewpoint of microstructural aspects are disputed.

**Keywords** crack paths, hydrogen embrittlement, transferability curve, fracture toughness, T-stress

## 1. Introduction

Fracture toughness is now considered as not intrinsic to material but depends on geometry, thickness, loading mode and more generally to constraint. Recent numerical and experimental studies have attempted to describe fracture in terms of two or three fracture parameters [1-3]. The elastic stress fields in a region surrounding the crack tip can be characterized by the following solution [1]:

$$\sigma_{ij} = \frac{K_I}{\sqrt{2\pi r}} f_{ij}(\theta) + T\delta_{xi}\delta_{xj} + A_3\sqrt{2\pi r} + 0(r) \quad (1)$$

where  $K_I$  is the stress intensity factor,  $f_{ij}(\theta)$  is the angular function,  $\delta_{ij}$  is the symbol of Kronecker's determinant. A polar coordinate system  $(r;\theta)$  with origin at crack tip is used. Several methods have been proposed in literature to determine the T-stress for cracked specimen. The stress difference method has been proposed by Yang et al. [4]. It was noted [5-8] that T-stress characterizes the local crack tip stress field for elastic linear material, and the elastic plastic material with the restriction of small-scale yielding conditions. Various studies have shown that T-stress has significant influence on fracture toughness, crack growth direction,  $A_3$  has some influence crack stability [9-15].

The K-T and K- $A_3$  approaches lead to a two-parameter fracture criterion. With K as the driving force and T or  $A_3$  a constraint parameters, a master failure curve can be successfully used to take into account the constraints of stress fields for various proposed geometry and loading structure configurations. Recently, the master curve has been evolved into a mature technology for characterizing the notch fracture toughness to quantify constraint effects for different testing specimen and structures [16].

The effect of T-stress on crack paths has been investigated for various specimen configurations and materials [17-19]. But some results of the crack path estimation give ambiguous data; for example, it was shown [20] that if the T-stress in front of a flat crack is negative then the crack grows along the crack plane. In the case of a positive T-stress, the crack deviates from its initial plane. It was also observed that the crack did not turn immediately when the T-stress became positive but at a considerably higher value. The method employed in Ref. [21,22] was developed for a kink which is formed at a given angle to the main crack [23]. Actual attention has been paid to problem of hydrogen pipeline systems due to strong world asking in energy and environmental problems. One future way is to use hydrogen as energy vector. In one European project [24], hydrogen transport will be provided way by adding hydrogen to natural gas in existing networks. Experience shows that the majority of pipeline failure initiates from defects or cracks [25-27]. Effects of transported hydrogen affect material mechanical properties, namely, hydrogen embrittlement [28,29]. The external environmental conditions cause free corroding processes, where hydrogen is product on metal surface as result of cathodic counterpart of the anodic dissolution reaction [30,31]. The gas pipeline industry recognizes this well as a major problem.

The aim of present work is to study the influence of hydrogen coupled with constraint (T stress is used as constraint parameter) on master failure curve and crack path direction and stability. In the first part the influence of hydrogen on master failure curve determined from fracture tests performed on different specimens geometries (CT, SENT, RT and DCB) has been studied. In a second part, fracture path under low constraint (negative T-stress) has been studied. Fracture has been obtained by burst tests under hydrogen pressure of pipes. In the third part, fracture path under high constraint (positive T-stress) has been studied from fracture of DCB specimens. Finally, a proposed mechanism of crack extension with constraint and hydrogen embrittlement has been proposed.

## 2. Material

The material used in this study is an X52 steel meeting requirements of API 5L standard. API X52 steel was the most common gas pipeline material for transmission of oil and gas during 1950-1960. Chemical composition of the studied steels is given in Table 1. In table 2, the mechanical properties of API X52 steel have been presented.  $E$ ,  $\sigma_y$ ,  $\sigma_u$ ,  $A\%$ ,  $n$ ,  $k$  and  $K_{Ic}$  are the Young's modulus, yield stress, ultimate stress, elongation at fracture, strain hardening exponent and hardening coefficient of Ramberg-Osgood law, and fracture toughness, respectively. Stress strain curves of X52 steel have been determined with and without hydrogen absorption and reported in Figure 1. Classical tensile properties such as yield stress and ultimate strength increases also when hydrogen is absorbed in steel as indicated in Table 2. A small increase of yield stress has been noted (2.5%) as an important reduction of elongation at failure (38%). Static stress-strain is obtained by fitted tensile test results using hardening power law  $\sigma = K \cdot \epsilon^n$ . Microstructure of API 5L X52 steel in the longitudinal and transverse orientation is shown in Figure 2 (a) and Figure 2 (b), respectively. These pictures show the distribution of the ferrite and pearlite with respect to orientation. The distribution of pearlite in

upper surface (Figure 2.a) appears to be relatively isotropic when compared to the pearlite bands in inner the surface (Figure 2.b). However, Figure 2 shows pearlite bands in different sections of the API 5L X52 specimen.

Table 1. Chemical composition of API X52 steel (weight %).

C	Mn	P	Si	Cr	Ni	Mo	S	Cu	Ti	Nb	Al
0.22	1.220	-	0.240	0.16	0.14	0.06	0.036	0.19	0.04	<0.05	.032

Table 2. Mechanical properties of API X52.

E, GPA	$\sigma_Y$ , MPa	$\sigma_u$ , MPa	A, %	n	K	$K_{Ic} MPa\sqrt{m}$
210	410	528	32	0.164	876	116.6

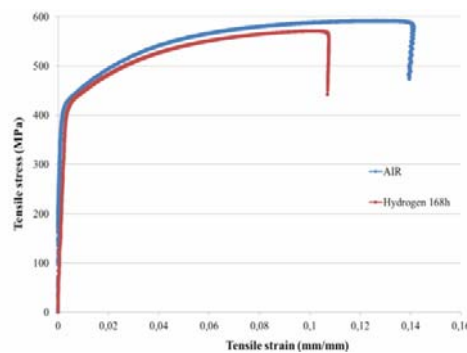


Figure 1. stress strain curves of X52 pipe steel with and without hydrogen absorption.

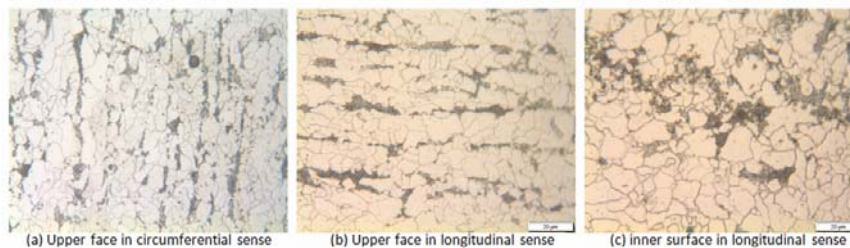


Figure 2. X52 metallographic sections showing ferrite-pearlite microstructure with bands (nital etching- originally taken at (a) 100x and (b) 500x)

### 3. Influence of Hydrogen on Master Failure Curve

Due to the assumptions, that pipes failure emanates mainly from external interferences i.e. that defect promoting failure are considered as notch, the notch fracture toughness (critical notch stress intensity factor)  $K_{\rho,c}$  and the critical effective T-stress ( $T_{ef,c}$ ) were employed to describe the material

failure curve  $K_{\rho,c} = f(T_{ef,c})$ . The critical notch stress intensity factor  $K_{\rho,c}$  is determined by the

Volumetric Method (VM) [32]. Averaging the T-stress distribution inside the effective distance (determined by Volumetric Method), the effective T-stress ( $T_{ef}$ ) can be defined in the following

form:

$$T_{ef} = \frac{1}{X_{ef}} \int_0^{X_{ef}} T_{xx}(r) \cdot \Phi(r) \cdot dr \quad (3)$$

$K_{\rho,c}-T_{ef,c}$  has been determined with [6] and without [2] the presence of hydrogen. Different specimens geometries (CT, SENT, RT and DCB) are used, all with a notch and a depth ratio of 0.5 ( $a/t = 0.5$ ). Specimens have been submitted to hydrogen environment during 30 days. Fracture initiation is detected by acoustic emission and provides load for crack initiation  $P_i$ , more details are given in [12]. Results are compared with results of [2] and summarized in Figure 3. The material master curve is approximated by the following equation

$$K_{\rho,c} = a T_{ef,c} + b \quad (4)$$

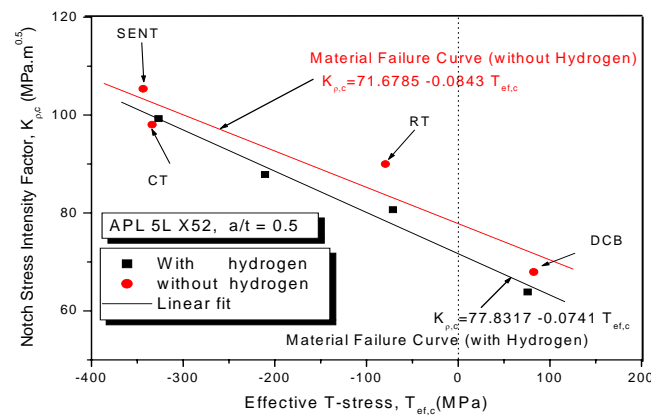


Figure 3. The experimental assessment points ( $K_{\rho,c}, T_{ef,c}$ ) and the material failure curve  $K_{\rho,c} = f(T_{ef,c})$  for X52 pipe steel with and without hydrogen effect [6].

where  $a = -0.0843$  and  $b = 71.6785$  for the X52 pipe steel without hydrogen embrittlement and  $a = -0.0741$  and  $b = 77.83$  for the X52 pipe steel with hydrogen embrittlement. One notes a small decreases of fracture toughness decreases in the range [5.8 %– 9.8 %] when  $T_{ef}$  increases in the range [- 400 MPa- +100 MPa] with a small difference for SENT specimen and larger for DCB specimen (about 10 %). One note a parallel with the decrease of fracture resistance in term of master failure curve and increase of the yield stress after hydrogen introduction. A small increase of yield stress has been noted (2.5%), as an important reduction of elongation at failure (38%). Also one notes that increasing the yield stress increases the constraint parameter.

## 4. Hydrogen and Constraint Effect on Kinking Direction

### 4.1 Fracture under low constraint

Fracture of pipe under internal pressure is performed under low constraint. Notched tubes were used for burst tests under pressure of hydrogen gas. Tubes were manufactured with steel X52, which

chemical composition, mechanical properties at elongation and environmental conditions of tests are given in [33].

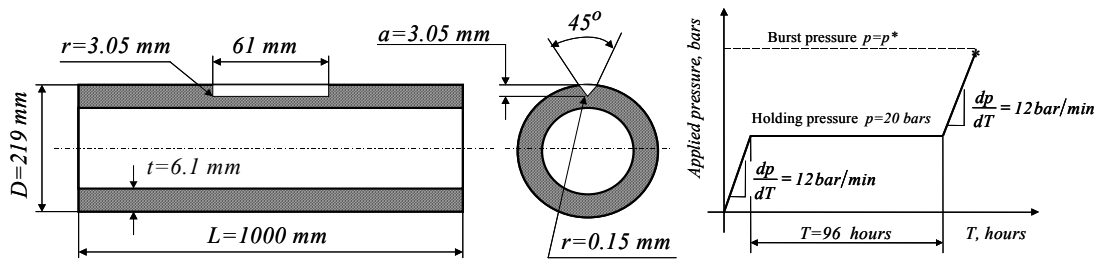


Figure 4. Tubes- Specimen for test

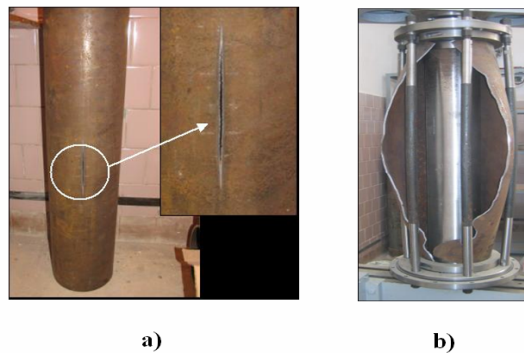


Figure 5. Burst tests of the model specimens made from Ukrainian tube:  
a - elastoplastic failure; b – catastrophic brittle fracture.

Tubes-specimens have a longitudinal notch on the outer surface and their geometry is given in Figure 4. Pipes were tested until burst according to the test sequence described in Figure 5. T-stress distribution indicates that T stress is negative and increases with internal pressure (see Fig.6). Test results showed that burst pressure for test in methane is equal  $p_{max} = 118 \text{ bar}$  and burst pressure for test in hydrogen is equal  $p_{max} = 122 \text{ bar}$ . Therefore, there is no gaseous hydrogen effect on the strength of notched pipes for considered testing conditions. At this critical pressure effective T-stress  $T_{ef}$  is equal to  $-22.268 \text{ MPa}$ . This negative value indicates a relatively low constraint.

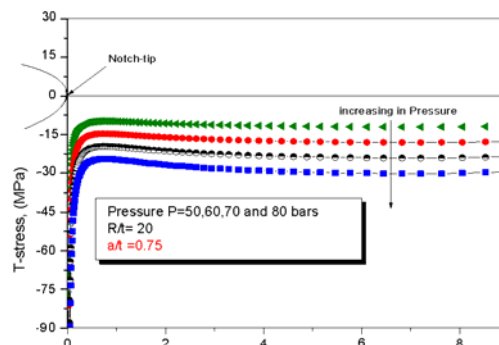


Figure 6. Evolution of T-stress versus distance over ligament. Pipe submitted to internal pressure.  
Diameter 400 mm thickness 10 mm (pressure 50-80 bars)

After burst tests, fracture surfaces were examined with a Scanning Electron Microscopy (SEM) for determination of fracture initiation points and also for checking of eventual fracture surface modification under influence of hydrogen. It has been found for hydrogen tests, inner fracture surface is characterized by an array of surface cracks (see Fig. 7-a). Careful examination shows that, surface cracks density is higher and average crack length is smaller. View of surface cracks under hydrogen conditions is given in Fig. 7.b at magnification X250.

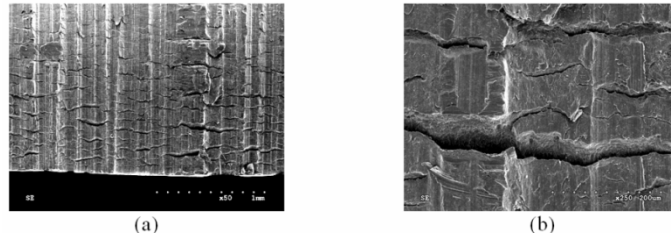


Figure 7. (a) surface cracks mesh at the edge of fractured notch for test in hydrogen. (b) magnification X250.

Examination of the notch bottom shows that fracture is originated at centre of notch ( $\pm 1$  at  $2\text{ mm}$ ). The mechanism of fracture initiation is developing of micro cracks from notch bottom (Fig. 7.a). Generally fracture surface consist of two parts. First part is a flat surface created by micro cracks growth from notch bottom and second part is final failure surface, which is made by shear mechanisms. This second part prevails at the inner surface of tube along notch and it may be considered as final ductile failure (Fig. 8.a). For test in hydrogen, the following aspect was observed. There is alternation of brittle and ductile sites of fracture character (Fig.8.b). The depth of particular surface aspect doesn't exceeds a distance of about  $50\ \mu\text{m}$  from notch bottom. No crack bifurcation was observed with or without hydrogen and this fact is considered as the result of fracture occurring under low constraint.

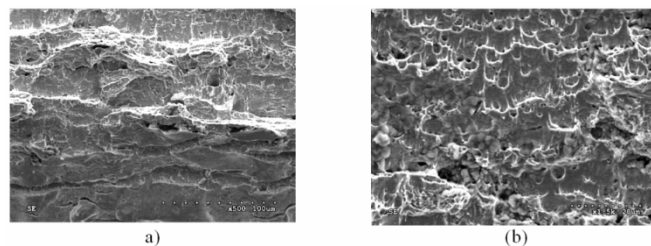


Figure 8. (a) Micro cracks at the notch bottom as source of fracture initiation for test in hydrogen. (b) fracture character at the inner surface.

#### 4.2 Fracture under high constraint

Fracture tests have been made on DCB specimen made in X52 steel. Geometry and dimensions of specimen is aregiven in figure (9).

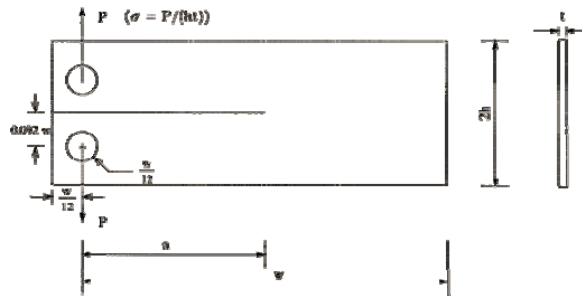


Figure 9. Geometry and dimensions of DCB specimens made in X52 steel.

Effective T stress has been determined by computed T stress distribution by Finite Element method along ligament and applying the Stress Difference Method, SDM [4]. Effective T stress distribution is presented in Figure 10. T is positive and indicates a low of constraint.  $T_{ef,c}$  at failure is equal to (+151.657 MPa). Observation of hydrogen effects by SEM on crack paths is shown in Figure 11 on CT and DCB specimens. Presences of hydrogen also induce another feature on crack growth that will contribute to the acceleration effect. A comparison is made with CT specimen which develops higher constraint. For CT in air and hydrogen crack grows perpendicular to the principal opening stress in mode I. For DCB under hydrogen, there is facility to extend crack in perpendicular direction and this could cause microscopic deviations in the crack path (Figure 11). These deviations can lead into crack branching or kinked crack paths [12].

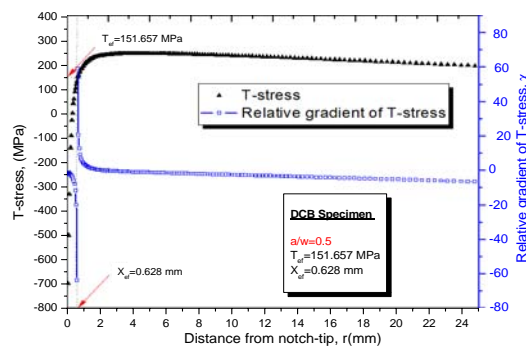


Figure 10. Evolution of the T-stress along of ligament for DCB specimen.

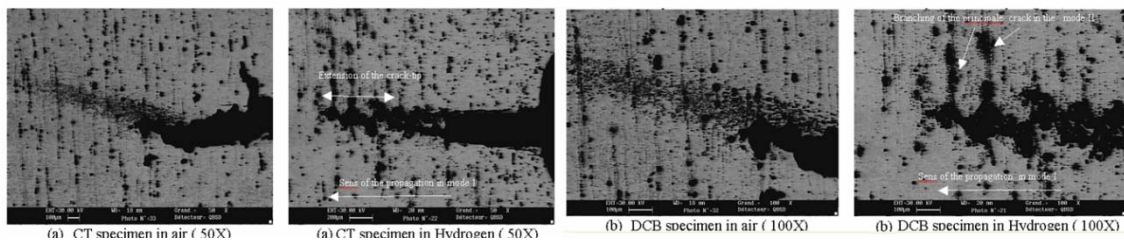


Figure 11. Observation by SEM of the cracks formation in pipeline during its service in different environments: air and hydrogen for CT and DCB specimens.

Crack propagation in air shows perlite debonding and ferrite matrix cracking as in Figure 12. In air, crack propagates by mode I in ferrite phase. Some cracks are arrested in the perlitic phase, and continue as second crack in ferrite. Extension of second crack, is probably prolongation of the first crack in third dimension. The perlite phase play the role of crack arrestator.

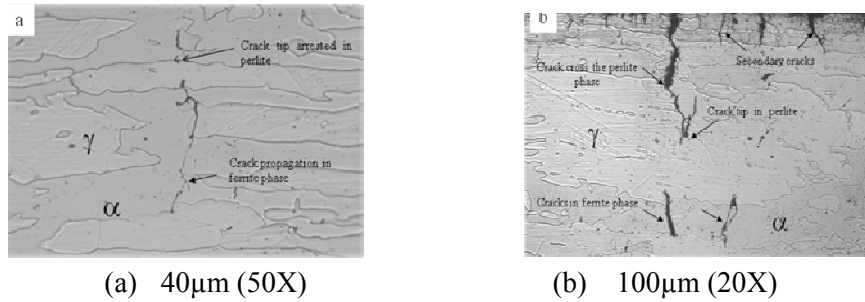


Figure 12. Optical photographs for cross section through the cracks and secondary cracks (a) –without hydrogen & (b) –hydrogen environment

With hydrogen environment, fracture is sometimes initiated from secondary cracks and very close to the surface due to pitting under hydrogen attack as shown in Figure 12.b. The crack stress field will produce a strain magnification in adjacent micro-cracks and penetration of hydrogen atoms will result in further cracking of ferrite phase at the crack tip. The crack cross the perlitic phase and will propagate in the straight direction, facilitating hydrogen propagation and weeping.

## 5. Discussion

It can be seen that critical effective  $T_{ef,c}$ -stresses have the influence on crack paths. Pipe submitted to internal pressure has higher negative critical value of the T-stress,  $T_{ef,c}$ , range and consequently lower constraint in comparison with bending specimens. SENT and CT specimens have also a high negative value of the  $T_{ef,c}$ -stress for cracks emanating from notch tip but lower than a notched pipe. For these specimens and pipe submitted to internal pressure, crack extension is observed along x direction, i.e. perpendicular to the principal tensile stress (Fig. 13.a). DCB specimens exhibits a particular positive  $T_{ef,c}$ -stress values ( Fig. 13.b). In this case, crack bifurcation appears after fracture initiation.

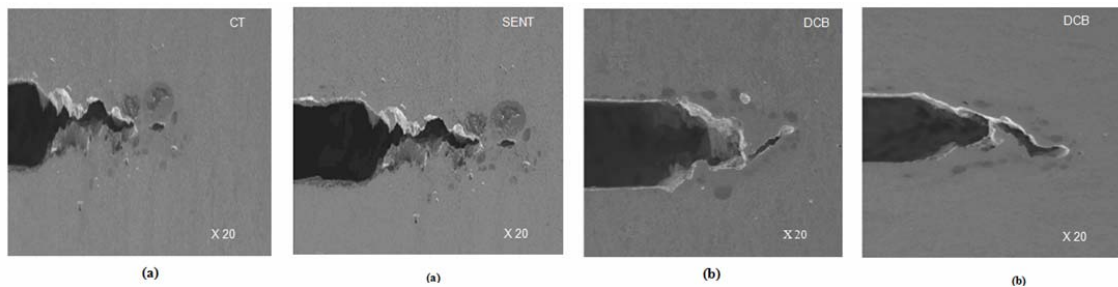


Figure 13. Kinking direction for (a) SENT and CT specimen, (b) DCB specimen.

Crack extension in API 5L X52 steel is governed by ductile failure mechanism, namely, nucleation of microvoids, growth and coalescence of these microvoids. However, pipe under internal pressure, CT, and SENT specimens, voids close to the notch are not elongated along the direction of loading but are elongated along shearing stress direction component which induced failure by mode II superimposed with mode I. Therefore, crack extension has a zigzag path characteristic of mixed mode (I + II failure mode). This zigzag mechanism can be seen on Figure 14.a with and without the hydrogen effect.

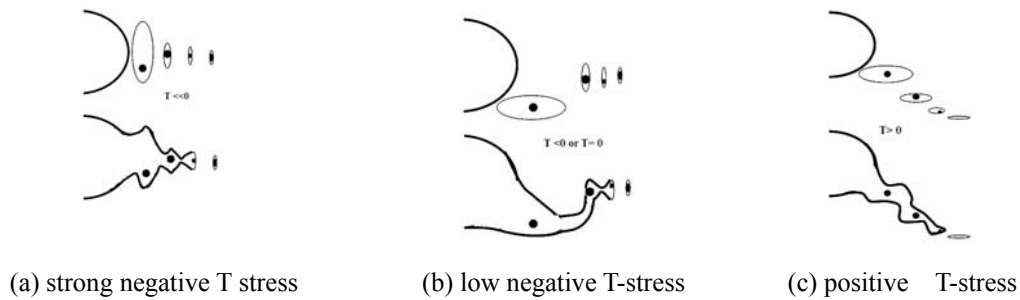


Figure 14. Proposed mechanisms for ductile crack extension under negative or positive  $T_{ef,c}$ -stresses.

For DCB specimen, the T-stress component is positive and voids are elongated closed to shearing direction. Crack path is linear along a direction which is close to pure mode II bifurcation angle ( $70^\circ$ ) (see Fig. 14.b). Therefore, ductile crack extension is governed by the intensity of shearing mode induced by the T-stress. Thus, the following model of crack extension can be assumed to describe crack paths as a function of the critical effective T-stress. Due to hard particles inside voids (these particles promote voids nucleation by stress concentration), voids cannot be closed by compressive (negative) T-stress and crack extension is then stable in notch direction according to scheme in [12]. If the T-stress is positive and higher than opening stress at some distance ahead of the notch tip, void extension then occurs in x direction which is corresponding to the maximum  $T_{ef,c}$ -stress direction. In this case, crack extension is made by bifurcation.

## 6. Conclusion

Fracture toughness is not really intrinsic to material but depend on constraint. The critical notch stress intensity factor versus the effective T stress build up a master curve which coupled the fracture driving force gives the critical conditions for any kind of geometry and loading mode. For the pipe steel API X52, the master curve exhibits a linear decreasing behavior. Slope and value at origin are few affected by hydrogen embrittlement. Crack path after fracture initiation is affected by constraint evaluated by T stress. A loss of constraint corresponds to high negative T effective value. This situation occurs in notched pipe submitted to internal pressure and crack path remains normal to maximum principal stress. This is unchanged after hydrogen embrittlement but fracture appearance is then modified. Over a short distance ahead of notch tip, there is a mixture of dimples and brittle facets. Fracture of DCB specimens occurs under high constraint characterized by a positive value of T stress. Crack kinking occurs due to mixed mode I +II induced by superposition of T stress. It has been seen on CT specimen with a lower constraint than DCB specimen that hydrogen embrittlement promotes this crack kinking. Further works are required to understand the shift of critical T effective value to promote crack kinking to lower value. The assumption of decreasing shearing mode cohesion energy with hydrogen will be investigated. Following the same idea, evolution of ratio of shearing and opening mode cohesion energy will be determined by appropriate experiments.

## References

1. Chao, Y.J., Liu, S., and Broviak, B.J. (1999). Variation of fracture toughness with constraint of PMMA specimens. *Proceedings of ASME-PVP* 393, 113–120.
2. Hadj Meliani M., Pluvinage G., Matvienko Y.G. (2011). Two Parameter Fracture Criterion ( $K_p-T_{ef}$ ) Derived From Notch Fracture Mechanics. *Internal Journal of Fracture*. 167:173–182.
3. M. Hadj Meliani, Z. Azari, G. Pluvinage, Y.G. Matvienko (2011). Variation of Material Failure Curve with Constraint. *Procedia Engineering*. **10**. 710-715.
4. Yang, B. Ravi-Chandar, K. (1999). Evaluation of elastic T-stress by the stress difference method. *Engng Fract Mech*. 64:589-605.
5. Chao Y.J., Liu S. and Broviak B.J. Brittle fracture (2011). variation of fracture toughness with constraint and crack curving under mode I conditions. *Experimental Mechanics*, 41, 3, pp 232-241.
6. Hadj Meliani M., Azari Z., Matvienko Y.G., Pluvinage G. (2011). The Effect of Hydrogen on the Material Failure Curve of APL 5L Gas Pipe Steels. *Procedia Engineering*. **10**. 942-947
7. Hadj Meliani M., Azari Z., Pluvinage G., Capelle J (2010). Gouge assessment for pipes and associated transferability problem. *Engng Failure Analysis*; **17**: 1117-1126.
8. Ayatollahi, M.R., Pavier, M.J., and Smith, D.J. (2002). Mode I cracks subjected to large T-stresses. *International Journal of Fracture* 117(2), 159–174.
9. Chao YJ, Reuter WG (1997). Fracture of surface cracks under bending loads. In: Underwood JH, MacDonald B, Mitchell M(eds) *Fatigue and fracture mechanics*, vol 28, ASTM STP 1321. American Society for Testing and Materials, Philadelphia, pp 214–242.
10. Sumpter, J.D.S (1993). An experimental investigation of the T stresses approach. *Constraint effects in Fracture*, ASTM STP 1171 (Edited by E. M. Hackett, K.-H. Schwalbe and R.H. Dodds), American Society for Testing and Materials, Philadelphia, 492-502.
11. Hancock, J.W, Reuter, W.G and Parks, D.M. (1993). Constraint and toughness parameterized by T. *constraint effects in Fracture*, ASTM STP 1171 (Edited by E.M. Hackett, K.-H. Schwalbe and R.H. Dodds), American Society for Testing and Materials, Philadelphia, 21-40.
12. Hadj Meliani M., Azari Z., Pluvinage G., Matvienko Y.G. (2011). The effective T-stress estimation and crack paths emanating from U-notches. *Engineering Fracture Mechanics*. 77(2010):1682–1692.
13. Hadj Meliani M., Azari Z., Pluvinage G. (2009). Constraint Parameter for a Longitudinal Surface Notch in a Pipe Submitted to Internal Pressure. *Key Engineering Materials. Advances in Strength of Materials*. Vol. 399 (2009) pp 3-11.
14. Hadj Meliani M., Benarous M., Moustabchir H., Harriri S., Azari Z. (2009). Three-dimensional T-stress to Predict the Directional Stability of Crack Propagation in a Pipeline with External Surface Crack. Springer Edition, Mars 2009.
15. Ayatollahi, M.R, Pavier, M.J, and Smith, D.J. (1998). Determination of T-stress from finite element analysis for mode I and mixed mode I/II loading. *Int. J. of Fracture* 91, 283-298.
16. Hadj Meliani M, Matvienko Yu.G, Pluvinage G (2011). Corrosion defect assessment on pipes using limit analysis and notch fracture mechanics. *Engng Failure Analysis*; **18**: 271-283.
17. Meshii T., Tanaka T(2010). Experimental  $T_{33}$ -stress formulation of test specimen thickness effect on fracture toughness in the transition temperature region. *Engineering Fracture Mechanics* **77** 867–877.

18. Matvienko Yu.G. (2011). A damage evolution approach in fracture mechanics of pipelines. In: Integrity of Pipelines Transporting Hydrocarbons, NATO Science for Peace and Security Series C: Environmental Security / eds.: G. Bolzon, T. Boukharouba, G. Gabetta, M. Elboudjaini and M. Mellas, Springer Netherlands: 227-244.
19. Maleski M.J., Kirigulige M.S. and Tippur H.V. (2004). A method for measuring Mode I crack tip constraint under dynamic and static loading conditions. Society for Experimental Mechanics, vol 44, N° 5.
20. Cotterell B, Rice JR(1980). Slightly curved or kinked cracks. Int J Fract; 16: 155-69.
21. Selvarathinam AS, Goree JG (1998). T-stress based fracture model for cracks in isotropic materials. EngFractMech; 60: 543-61.
22. Sumi Y, Nemat-Nasser S, Keer LM (1985). On crack path stability in a finite body. EngFractMech; 22: 759-71.
23. Cotterell B (1980). Notes on fracture paths and stability of cracks. EngFractMech; 13: 526-33.
24. European project. NaturalHy Project, <http://www.naturalhy.net>
25. Hadj Meliani M., Moustabchir H., Azari Z. (2007). T-stress by stress difference method (SDM): Numerical analysis on mode (I) loading. Particle and continuum aspect of mesomechanics. Mesomechanics 2007, Lille, France. p 253-260, edited by ISTE publishing Knowlge.
26. Sofronis P. and Lufrano J.(1999). Interaction of local elastoplasticity with hydrogen: embrittlement effects. Materials Science and Engineering, A260, pp. 41-47.
27. Eliezer D., Eliuaz N., Senkov O. N., Froes F. H (2000). Positive effects of hydrogen in metals. Materials Science and Engineering, A280, pp. 220-224.
28. Wilkowski G. (2000). Leak-before-break: what does it really mean? Journal of Pressure Vessel Technology, Transaction of ASME. Vol. 122, No 3, pp. 267-272.
29. Liu Y. H. Cen Z. Z., Chen H. F., Xu B. Y. (2000). Plastic collapse analysis of defective pipelines under multi-loading systems. International Journal of Mechanical Science. Vol. 42, pp. 1607-1622.
30. Hanneken J. W. (1999). Hydrogen in metals and other materials: a comprehensive reference to books, bibliographies, workshops and conferences, International Journal of Hydrogen Energy, Vol. 24, No 10, pp. 1005-1026.
31. Capelle J, Gilgert J, Dmytrakh I, Pluvinage G.( 2008). Sensitivity of pipelines with steel API X52 to hydrogen embrittlement. Int J Hydrogen Energy; **33**: 7630-7641.
32. Capelle J., Gilgert J., Dmytrakh I., Pluvinage G. (2011) . The effect of hydrogen concentration on fracture of pipeline steels in presence of a notch. Engineering Fracture Mechanics **78**;364–373.
33. Naturalhy-Project(2005). Burst tests on pipes under pressure of mixture of hydrogen and natural gaz. Contract N° SES6/2004/502661.Durability and Integrity Work-packages. Subcontract N° 1401-2005.